Limitation of absorption-based fiber optic gas sensors by coherent reflections

W. Jin, G. Stewart, W. Philp, B. Culshaw, and M. S. Demokan

We report the noise limitation of fiber optic gas sensors with highly coherent laser sources. Interference between signal and reflected waves causes signal fluctuation in the output; this limits the performance of the sensing system. Sensor resolutions limited by coherent reflections are calculated and compared with experimental results. © 1997 Optical Society of America

Key words: Fiber optic sensors, gas sensors, coherent reflections, interferometric noise.

1. Introduction

Optical gas sensors based on absorption of light by the vibrational–rotational energy levels of gas molecules at near-IR (1–1.8-μm) wavelength have attracted considerable attention recently.[1–4] The advantages of fiber sensors are remote detection capability, safety in hazardous environments, immunity to electromagnetic fields, etc. The possible gases that can be detected are methane, acetylene, hydrogen sulphide, carbon dioxide, carbon monoxide, etc. Like other types of fiber sensors, the performance of gas sensors is limited by various kinds of noise: source, shot, thermal, etc. We have already reported the results of an investigation on the effect of source, shot, and thermal noises on the performance of a gas sensor that used a low-coherence optical source.[5] Gas sensors with highly coherent sources such as distributed feedback (DFB) and fiber lasers are advantageous for obtaining high sensitivity. However, for this type, interferometric noises caused by interference between signal and reflected waves might be larger than the source and detector noise and thus might set a limit on the sensor performance. In this paper, we report the performance limitation caused by coherent reflections in fiber gas sensors with highly coherent laser sources. The magnitude of the noise caused by reflections is estimated. The results of our investigation will help design engineers to understand the noise processes involved and to estimate the expected performance of a particular fiber optic gas-sensing system.

2. System Description

The basic principle of absorption-based gas detection by a laser is shown in Fig. 1 in which a transmission-type sensor is illustrated. When a laser beam of frequency ω and intensity I_0 passes through a gas sample, the output intensity $I(\omega)$ may be expressed as

$$I(\omega) = I_0 \exp[-2\alpha(\omega)CL], \tag{1}$$

where $\alpha(\omega)$ represents the attenuation coefficient in amplitude due to gas absorption, C is the gas concentration in terms of a fraction of pure gas. L is the distance during which the laser light interacts with the gas.

It is well known that the spectral line of a gas under atmospheric pressure is collision broadened, for which the line shape is given by the Lorentzian distribution. Therefore the absorption coefficient $\alpha(\omega)$ can be expressed as

$$\alpha(\omega) = \frac{\alpha_0}{1 + \left(\frac{\omega - \omega_0}{\delta\omega}\right)^2}, \tag{2}$$

where α_0 is the absorption coefficient at ω_0 corresponding to the center of the absorption line (maximum absorption) and $\delta\omega$ is the half-width at half-maximum (HWHM) of the absorption line.

The two most commonly used techniques for gas detection are differential absorption spectroscopy and frequency modulation spectroscopy. They are

W. Jin and M. S. Demokan are with the Department of Electrical Engineering, The Hong Kong Polytechnic University, Hung Hom Kowloon, Hong Kong. G. Stewart, W. Philp, and B. Culshaw are with the Department of Electronic and Electrical Engineering, University of Strathclyde, Glasgow G1 1XW, UK.

Received 16 September 1996; revised manuscript received 27 November 1996.

0003-6935/97/256251-05$10.00/0

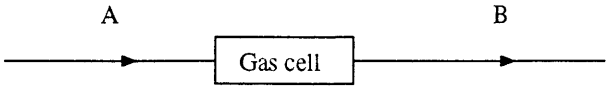

Fig. 1. Principle of absorption spectroscopy.

more or less based on the same fundamental principle, namely, comparison of the output light intensities at different wavelengths. Considering differential absorption spectroscopy, the system output is the ratio of the light intensity at two distinct wavelengths, one (with intensity I_1) at the center of the absorption peak, and two (with intensity I_2) displaced from the center to a position where the absorption is small and might be neglected. The system output may be expressed as

$$\frac{I_1}{I_2} = \exp(-2\alpha_0 CL). \tag{3}$$

The ratio detection method eliminates intensity fluctuation due to factors other than gas absorption.

If there are errors in the measurement of I_1 and I_2, i.e., $I_{1m} = I_1 + \Delta I_1$ and $I_{2m} = I_2 + \Delta I_2$, or $I_{1m} = I_1(1 + \delta_1)$ and $I_{2m} = I_2(1 + \delta_2)$, where $\delta_1 = (\Delta I_1/I_1)$ and $\delta_2 = (\Delta I_2/I_2)$ represent relative measurement errors; the measured value of gas concentration (C_m) would be different from the real value of gas concentration (C). C_m and C may be related by the following equation:

$$\begin{aligned}\frac{I_{1m}}{I_{2m}} &= \exp(-2\alpha_0 C_m L),\\ &= \frac{I_1(1+\delta_1)}{I_2(1+\delta_2)}\\ &\approx \exp(-2\alpha_0 CL)(1+\delta_1-\delta_2),\end{aligned} \tag{4}$$

where m represents the measured values and we have assumed that δ_1 and δ_2 are small so that

$$\frac{1+\delta_1}{1+\delta_2} \approx 1 + \delta_1 - \delta_2. \tag{5}$$

Rearranging Eq. (4), we have

$$\exp[2\alpha_0(C - C_m)L] = 1 + \delta_1 - \delta_2. \tag{6}$$

For small measurement errors, we may use the approximation $\ln(1 + x) \approx x$ and obtain

$$2\alpha_0(C - C_m)L \approx \delta_1 - \delta_2. \tag{7}$$

The maximum error in gas concentration can then be expressed as

$$|\Delta C| = |C - C_m| \le \frac{|\delta_1| + |\delta_2|}{2\alpha_0 L}. \tag{8}$$

Take an absorption-based methane sensor at 1665.5 nm (Q6 line) as an example. Under atmospheric pressure, $2\alpha_0 \approx 0.2\ \text{cm}^{-1}$, and for a 10-cm cell ($L = 10$ cm), we have $2\alpha_0 L \approx 2$. So to achieve 10-ppm accuracy ($\Delta C < 10$ ppm) requires $|\delta_1| + |\delta_2|$ to be less than -47 dB.

For modulation spectroscopy, the laser wavelength is continuously tuned in a sinusoidal manner around the center of the absorption line, and, because of the variation of absorption with wavelength, this modulation of wavelength is converted into an intensity variation. For frequency modulation spectroscopy based on current modulation of a DFB laser, the system output often takes the ratio of a second harmonic and a first harmonic, in which the former is proportional to gas concentration and the latter is used as a reference to remove intensity fluctuations from effects other than gas absorption. For this technique, the measurement error can still be estimated by use of Eq. (8), but δ_1 and δ_2 represent measurement errors in the amplitudes of the first harmonic and the second harmonic, respectively.

In this paper, we investigate the characteristics of interferometric noise due to reflections for a system with differential absorption spectroscopy. For frequency modulation spectroscopy, the analysis is considerably more complicated, but the results reported here give a useful indication of the order of magnitude of the noise from coherent reflections and for a general fiber gas-sensing system.

3. Coherent Reflections in Transmission-Type Sensors

For transmission-type sensors (see Fig. 2), while the first-order reflection will be directly fed back into the source, we may assume that they have no effect on the system performance when a proper isolator is used at the laser output port. The second-order reflection (reflection caused by a pair of reflective points

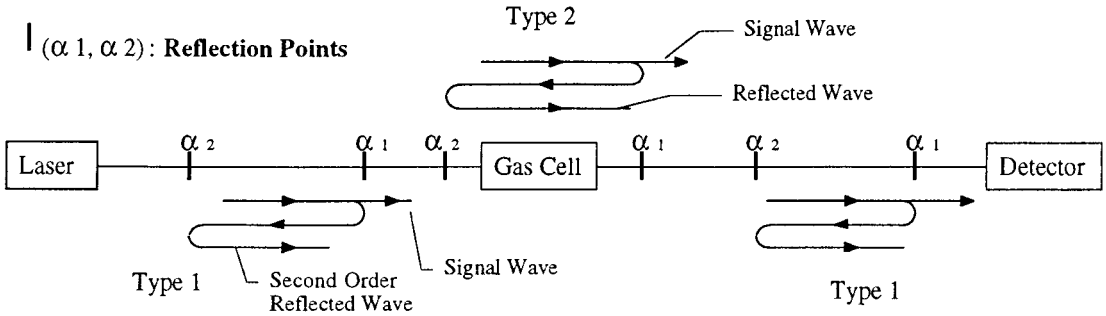

Fig. 2. Second-order reflection pairs in a transmission-type sensor.

along the fiber, first backward then forward; see Fig. 2), however, might affect the system performance. In the output of the system, in addition to a primary beam, many second-order waves due to second-order reflections may exist. Reflections can occur at fiber connectors, fiber-cell joints (cell surfaces), etc. For simplicity, we divide the reflections into two types as shown in Fig. 2.

A. Reflection Pairs before or after the Cell (Type I)

Signal wave (at output detector):

$$E(t) = E_0 \exp[-\alpha(\omega)CL]\exp(j\omega t). \quad (9)$$

Reflected wave (at output detector):

$$\begin{aligned} E_r(t) &= \alpha_1\alpha_2 E(t-\tau) \\ &= \alpha_1\alpha_2 E_0 \exp[-\alpha(\omega)CL]\exp[j\omega(t-\tau)], \end{aligned} \quad (10)$$

where $E_0 = \sqrt{I_0}$ is the amplitude of the laser field, α_1 and α_2 represent the amplitude reflection coefficients at two points as shown in Fig. 2, τ is a time delay between the primary and the reflected wave.

The total light intensity at the output detector $I(t)$ may be divided into three parts, the intensity of the signal wave, the intensity of the reflected wave, and the mixing between the signal and the reflected wave. The intensity of the reflected wave is of a higher order compared with the other two terms and can be neglected. In this paper, we will consider only two terms: the signal and the mixing term (noise term), which induces errors in the measurement.

Signal intensity:

$$I_s = \langle |E(t)|^2 \rangle = {E_0}^2 \exp[-2\alpha(\omega)CL]. \quad (11)$$

Noise intensity:

$$\begin{aligned} I_n &= 2\mathrm{Re}\langle E(t)E_r^*(t)\rangle \\ &= 2\alpha_1\alpha_2|\gamma(\tau)|{E_0}^2 \exp[-2\alpha(\omega)CL]\cos(\omega\tau), \end{aligned} \quad (12)$$

where $\gamma(\tau)$ is coherence function of source.

The measurement error δ_1 and δ_2 (caused by coherent reflections) can then be expressed as

$$\delta_i = \frac{I_n}{I_s} = 2\alpha_1\alpha_2|\gamma(\tau)|\cos(\omega_i\tau), \quad (13)$$

where $i = 1, 2$ corresponds to a different wavelength. The measurement error is dependent on the reflection coefficients α_1 and α_2, and time delay τ between the reflected and the signal waves. Because of variation of temperature and other environmental factors, τ changes randomly with time, causing δ_1 and δ_2 to change with time. The maximum values of δ_1 and δ_2 may be written as

$$|\delta_1|_{\max} = |\delta_2|_{\max} = 2\alpha_1\alpha_2|\gamma(\tau)|. \quad (14)$$

Note that the maximum error depends on the relative positions of the reflection points and the coherence function of the source; if the two reflection points are situated so that the time delay (τ) between the reflected and the signal wave is much longer than the coherence time of the source, the measurement error δ_1 and δ_2 will be greatly reduced.

For multiple pairs of reflection points, if we assume that the cross interference between the different secondary waves is small and can be neglected, the signal intensity remains approximately the same, but the noise intensity is a summation of contributions from all the pairs of reflection points.

B. Reflection Pairs across the Cell (Type II)

For the case of a pair of reflection points, one before and after the cell (see Fig. 2), the reflected wave can be written as

$$E_r = \alpha_1\alpha_2 E_0 \exp[-3\alpha(\omega)CL]\exp[j\omega(t-\tau)]. \quad (15)$$

The signal intensity is the same as that in Eq. (11), and the interfering term can be written as

$$I_n = 2\alpha_1\alpha_2|E_0|^2 \exp[-4\alpha(\omega)CL]|\gamma(\tau)|\cos(\omega\tau). \quad (16)$$

For example, considering reflections from the surfaces of the gas cells, α_1 and α_2 will be the reflection coefficient of the cell surfaces and τ will be the round-trip delay of the gas cell (cavity).

The relative error δ_1 and δ_2 can be calculated as

$$\delta_1 = \frac{I_n}{I_s} = 2\alpha_1\alpha_2 \exp(-2\alpha_0 CL)|\gamma(\tau)|\cos(\omega_1\tau), \quad (17)$$

$$\delta_2 = 2\alpha_1\alpha_2|\gamma(\tau)|\cos(\omega_2\tau), \quad (18)$$

where δ_1 and δ_2 changes with environment due to changes in τ with say temperature. It might be necessary to choose low-thermal expansion material to improve the stability of the system. At the worst case, the maximum error $|\delta_1|_{\max}$, $|\delta_2|_{\max}$ can be written as

$$|\delta_1|_{\max} = 2\alpha_1\alpha_2|\gamma(\tau)|\exp(-2\alpha_0 CL), \quad (19)$$

$$|\delta_2|_{\max} = 2\alpha_1\alpha_2|\gamma(\tau)|. \quad (20)$$

Again, if there are multiple reflection points across the cell, the summation of contributions from all possible pairs should be considered. The total measurement error of the whole system will be the summation of contributions from all the type I and type II reflections. The measurement error $|\Delta C|$ can be estimated by use of Eqs. (14), (19), (20), and (8).

4. Coherent Reflections in Reflective-Type Sensors

So far, most of the reported gas sensors with laser sources are of the transmission type. However, the reflection type is also possible and might be advantageous because it requires only a single transmission fiber. In this section, we study the noise limit of reflective-type sensors set by coherent reflections.

In reflective-type sensors as shown in Fig. 3, the first-order reflections begin to seriously limit the system performance. Even though the incidence of the reflected waves together with the returned signal on the laser is prevented by the use of an isolator following the laser, the mixing between the first-order

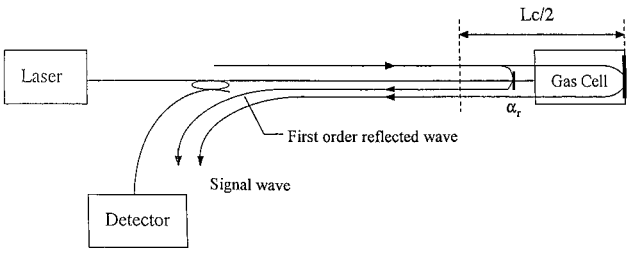

Fig. 3. First-order reflection in a reflective-type sensor.

reflected waves and the signal wave at the detector causes significant measurement errors.

Not all the reflected waves (first order) can interfere with the signal wave. Only those reflections from particular sections of the fiber, which travel nearly the same length (within a coherence length L_c) as the signal wave contribute to the noise. (Figure 3 shows a reflected wave from one reflection point.) Reflections near the gas cell have a major effect.

Similar to the treatment in the proceeding section, the signal wave $E(t)$ is given by Eq. (9) and the reflected wave $E_r(t)$ can be written as

$$E_r = \alpha_r E_0 \exp[j\omega(t - \tau_r)], \tag{21}$$

where τ_r represent the delay of the reflected wave relative to the signal wave; α_r is a reflection coefficient. L equals twice of cavity length of the gas cell because of the light that travels through the gas cell twice.

At the receiver, the signal intensity is given by Eq. (11) and the noise intensity can be written as

$$I_n = 2\alpha_r |E_0|^2 \exp[-\alpha(\omega)CL]\gamma(\tau_r)\cos(\omega\tau_r). \tag{22}$$

The measurement error δ_1 and δ_2 can then be expressed as

$$\delta_1 = 2\alpha_r \exp(\alpha_0 CL)\gamma(\tau_r)\cos(\omega\tau_r), \tag{23}$$

$$\delta_2 = 2\alpha_r \gamma(\tau_r)\cos(\omega\tau_r). \tag{24}$$

The maximum values of δ_1 and δ_2 can then be written as

$$|\delta_1|_{\max} = 2\alpha_r \exp(\alpha_0 CL)|\gamma(\tau_r)|, \tag{25}$$

$$|\delta_2| = 2\alpha_r |\gamma(\tau_r)|. \tag{26}$$

Equations (8), (25), and (26) can be used to estimate the sensor resolution caused by first-order coherent reflection in a reflective-type system.

For a reflective-type sensor, in addition to the first-order reflections, second-order reflections also contribute to the measurement error. The mixing between the second-order reflected waves can be analyzed in the same way as in the transmission-type sensors. If all other conditions are the same (reflection points, coefficients, interaction length, etc), the measurement error produced by these second-order effects should be comparable with that of the transmission-type sensors.

5. Discussion

In the analysis presented in Sections 3 and 4, we have actually assumed that the polarization states of the signal and the reflected waves are the same. In a practical system, however, the polarization states of the signal and the reflected waves might be different and might change randomly with environmental disturbances. The effect of the different polarization states is to reduce the magnitude of the mixing term as given by Eqs. (12), (16), and (22), which in turn reduces the magnitude of the relative error δ_1 and δ_2. Indeed the measurement errors δ_1 and δ_2 can be reduced to zero if the polarization states of the signal and the reflected wave are orthogonal. Therefore Eqs. (13), (19), (20), (25), and (26) should be regarded as worst-case errors that can be reached only when the signal and reflected waves have the same polarization states.

As the sensing system is characterized by multipath, laser phase noise will be converted into intensity noise, which can play a role as one of the limiting noise factors. The amount of laser-phase-induced noise power in the detected output intensity is a function of center frequency and bandwidth of the detection system and is also dependent on the phase bias and time-delay difference between the interfering beams (the signal and the reflected waves as shown in Figs. 2 and 3) and the coherence time of the light source.[7] However, in any case, the ratio of laser-phase-induced intensity noise power and the power of the interferometric noise due to coherent reflections as discussed in Sections 3 and 4 is found to be less than $B\tau_c$[7]. Here B is the bandwidth of the detection system and τ_c is the coherence time of the source. If we assume a DFB laser of linewidth 50 MHz, and a detection bandwidth of up to 50 kHz, $B\tau_c$ should be $<10^{-3}$, indicating that the laser phase noise contribution is much less than the interferometric noise caused by coherent reflections.

6. Comparison of Two Types of Sensor and Comparison with Experimental Results

In Sections 3 and 4, we derived formulas for estimating sensor resolution as limited by coherent reflection for both transmission- and reflective-type sensors. In this section, we estimate the practical achievable limit of a particular type of sensor, i.e., a methane gas sensor based on absorption near a wavelength of 1665 nm. We assume that $L = 10$ cm, which corresponds to a 10-cm-long gas cell for a transmission-type sensor and a 5-cm-long gas cell for a reflective-type sensor, and use the Q(6) absorption line at wavelength 1665.5 nm. The absorption coefficient at this wavelength is $2\alpha_0 = 0.2\ \text{cm}^{-1}$ giving $2\alpha_0 L = 2$. From Eq. (8), we may express the measurement error as

$$\Delta C = \frac{1}{2}(|\delta_1| + |\delta_2|), \tag{27}$$

where ΔC represents measurement error in terms of the fraction of pure methane at atmospheric pressure.

For transmission-type sensors and for reflection

pairs before or after the cell (type I reflections), if we assume the reflection coefficients are approximately the same, i.e.,

$$\alpha_1 = \alpha_2 = \alpha, \tag{28}$$

we obtain

$$|\delta_1|_{\max} = |\delta_2|_{\max} = 2\alpha_1\alpha_2 = 2\alpha^2; \tag{29}$$

therefore

$$|\Delta C|_{\max} \simeq 2\alpha^2. \tag{30}$$

The measurement error in gas concentration is proportional to the reflection coefficient. For a conventional fiber cable with FC/PC connectors, the (power) reflection at the joint is of the order of -40 dB ($\alpha^2 = 10^{-4}$), which corresponds to an error in methane concentration of 200 ppm.m. In other words, if we require a resolution of 10 ppm, the required power reflection coefficient should be 5 ppm = -53 dB. This may be obtained through use of either a continuous fiber or FC/APC rather than conventional FC/PC connectors. Note that the above value is for the worst case, where the two reflection points are so close that the time delay between the reflected light and the primary light is less than the coherence length of the source. If the distance between the two reflection points is well beyond the coherence length, the measurement error is greatly reduced. Usually, fiber joints in the transmission system can be made to be well beyond the coherence length, but multiple reflections near the source and/or detector modules need to be carefully considered.

The reflections occurring across the cell are probably due to reflections from the cell surfaces. Since the cell length is normally short compared with the coherence length of the source, we can almost certainly assume that $|\gamma(\tau)| = 1$ and the measurement error in gas concentration can then be calculated, by use of Eqs. (8), (19), and (20), as

$$|\Delta C| = \alpha^2[1 + \exp(-2\alpha_0 CL)]. \tag{31}$$

The error depends on the methane concentration C. At a small methane concentration so that $\alpha_0 CL \ll 1$, the error takes the same form as Eq. (30). Take a methane sensor with a gas cell formed with paired GRIN lenses (NSG Europe) of -30-dB backreflectance, the calculated sensor resolution by use of Eq. (30) is 200 ppm.m. This value agrees very well with our recent experimental data ($\sim$200 ppm.m) obtained with a setup as shown in Fig. 2.[6] Reduction of the reflection coefficient from the cell surface should yield high-accuracy measurement. For example, to obtain 1-ppm.m accuracy, the reflection coefficient should be <-53 dB. This can be achieved with antireflection coating and angled cell surfaces.

For reflective-type sensors, the second-order reflection induced error should be of the same order as that of a transmission-type sensor. The sensor resolution limited by first-order reflections can be estimated from Eqs. (8), (25), and (26), as

$$\Delta C = \alpha_r[1 + \exp(\alpha_0 CL)]. \tag{32}$$

It can be seen that the first-order noise increases with methane concentration in an exponential manner. The maximum error is obtained when $C = 1$ (pure methane). At small methane concentration $C \approx 0$ for a reflection coefficient (power coefficient) of $\alpha_r^2 = 10^{-4}$, the measurement error in C can be estimated from Eq. (32) as $2 \times 10^{-2} = 2\%$ methane. This is 2 orders of magnitude larger than the error in transmission-type sensors.

7. Summary

We have investigated interference induced noises in optical fiber gas-sensing systems with coherent sources such as DFB lasers. It was found that in a reflection-type sensor, the measurement error caused by first-order coherent reflections is 2 orders of magnitude larger than that in transmission-type sensors. The latter is limited by the second-order reflections.

For transmission-type sensors with FC/PC connectors with back reflection of -40 dB, or cavity reflection of the same order, the system limited performance is 200 ppm for a 10-cm cell or 20 ppm.m. This agrees with the experimental results that we obtained.

For reflective-type sensors, the main contribution is from first-order reflections. For reflection of the order of -40 dB, the first-order reflection effects have a magnitude of 2000 ppm.m. The magnitude of the second-order effects for a reflective-type sensor is similar to that of the transmission-type sensor.

References

1. H. Tai, K. Yamamoto, S. Osawa, and K. Uehara, "Remote detection of methane using a 1.65 μm diode laser in combination with optical fibers," in *Proceedings of the Seventh Optical Fiber Sensors Conference* (IREE, Sydney, 1990), pp. 51–54.
2. K. Yamamoto, H. Tai, M. Uchida, S. Osawa, and K. Uehara, "Long distance simultaneous detection of methane and acetylene by using diode lasers in combination with optical fibers," in *Proceedings of Eight Optical Fiber Sensors Conference* (IEEE, New York, 1992), pp. 333–336.
3. V. Weldon, P. Phelan, and J. Hegarty, "Methane and carbon dioxide sensing using a DFB laser diode operating at 1.64 μm," Electron. Lett. **29,** 560, 561 (1993).
4. Y. Shimose, T. Okamoto, A. Maruyama, M. Aizawa, and H. Nagai, "Remote sensing of methane gas by differential absorption measurement using a wavelength-tunable DFB LD," IEEE Photon. Technol. Lett. **3,** 86–87 (1991).
5. W. Jin, G. Stewart, and B. Culshaw, "Source noise limitation in an optical methane detection system using a broadband source," Appl. Opt. **35,** 2345–2349 (1995).
6. W. R. Philp, W. Jin, A. Mencaglia, G. Stewart, and B. Culshaw, "Interferometric noise frequency modulated optical gas sensors," in *ACOFT '96, 21st Australian Conference on Optical Fiber Technology* (IREE, Sydney, 1996), pp. 185–188.
7. B. Moslehi, "Noise power spectra of optical two-beam interferometers induced by the laser phase noise," J. Lightwave Technol. **LT-4,** 1704–1710 (1986).